Melting and crystallization of ultra-high-molecular-weight polyethylene in a mixture with tetracontane under high pressure

Chitoshi Nakafuku and Hitoshi Nakagawa
Faculty of Education, Kochi University, Kochi 780, Japan

Munehisa Yasuniwa and Shinsuke Tsubakihara
Department of Applied Physics, Faculty of Science, Fukuoka University, Jonan-ku, Fukuoka 814-01, Japan
(Received 5 January 1990; revised 28 February 1990; accepted 12 March 1990)

The melting and crystallization processes of ultra-high-molecular-weight polyethylene (UHMW PE) in a mixture with tetracontane (TC) were studied at elevated pressures up to 500 MPa by high-pressure differential thermal analysis. At atmospheric pressure, melting-point depression of UHMW PE occurs with increasing TC content, but it does not occur at 500 MPa. The phase transition to the hexagonal phase of UHMW PE is impeded by the addition of TC, and does not occur below a weight fraction of PE equal to 0.4 at 500 MPa. The content of extended chain crystals (ECC) of UHMW PE formed by high-pressure crystallization decreases with TC, and below a weight fraction of PE equal to 0.35, ECC do not form even on crystallization at 500 MPa.

(Keywords: polyethylene; ultra-high molecular weight; tetracontane; binary mixture; high pressure; melting; crystallization; differential thermal analysis; phase diagram; extended chain crystals)

INTRODUCTION

The melting and crystallization behaviours of polyethylene (PE) under high pressure have been studied for the past two decades. On heating, a phase transition from the orthorhombic phase to the hexagonal phase (high-pressure phase) occurs below the melting temperature under high pressure above ~ 350 MPa[1-15]. The high-pressure crystallization of medium-molecular-weight PE (MMW PE) ($MW = 10^4$–10^5) from the molten state produces so-called extended chain crystals (ECC)[16-24].

In a recent study[25], we reported that tetracontane (C_{40}) (TC) affects the phase transition and the formation of ECC of MMW PE ($MW = 6.7 \times 10^4$) under high pressure. That is, the high-pressure phase shifts to higher pressure and temperature with TC content in the mixture, and the high-pressure phase disappears when the weight fraction of PE (W_{PE}) is less than 0.7 at 500 MPa. At atmospheric pressure the melting temperature of the pressure-crystallized PE decreased with decreasing W_{PE}, and ECC are not formed below $W_{PE} = 0.5$ on crystallization even at 500 MPa.

We studied[26] the molecular-weight dependence of the melting and crystallization processes of PE under high pressure for the molecular-weight range from 10^3 to 2.5×10^6. It was shown that the high-pressure phase appeared for a powder sample of ultra-high-molecular-weight PE (UHMW PE) ($MW = 2.5 \times 10^6$). The high-pressure crystallization of UHMW PE was studied by high-pressure d.t.a. and scanning electron microscopy[27,28]. It has been reported that crystals like fibrous bands, with a melting temperature higher than ECC of MMW PE, were formed.

The effects of paraffins on the melting[10,29] and crystallization[30] of MMW PE have been studied at atmospheric pressure. Melting-point depression of PE occurs in mixtures with normal paraffins, such as hexatriacontane (C_{36}) and octadecane (C_{18})[10,29]. The melting and crystallization processes of UHMW PE under high pressure are interesting, because the region of the high-pressure phase changes with the molecular weight of PE and its sample preparation method at atmospheric pressure[26]. The orthorhombic–hexagonal transition temperature in UHMW PE with many entanglements induced by kneading shifted to lower temperature than that of UHMW PE powder sample with fewer entanglements. The entanglements increase with the molecular weight, especially in the ultra-high-molecular-weight region. Therefore, under high pressure it is expected that different melting and crystallization behaviours occur between MMW PE and UHMW PE in mixtures with tetracontane.

In this paper, the effect of TC on the melting and crystallization processes of UHMW PE under high pressure is studied by high-pressure d.t.a. The paraffins with lower carbon number than TC show complicated melting behaviour due to the rotator phase transition below the melting temperature. The pressure dependence of the phase diagram of the UHMW PE and TC binary mixture is determined. The effect of TC on the formation of ECC of UHMW PE under high pressure is also studied by d.s.c. at atmospheric pressure. The melting and

0032-3861/91/040696-07

crystallization behaviours of UHMW PE in the mixture under high pressure are compared with those of MMW PE in the mixture.

EXPERIMENTAL

Commercial-grade UHMW PE (Hizex 240M, $MW = 1.9 \times 10^6$) and MMW PE (Hizex 2200 JP, $MW = 6.7 \times 10^4$) supplied by Mitsui Petrochemical Industries Co. were used in this study. TC was purchased from Tokyo Chemical Industry Co. Ltd. Original powder samples of UHMW PE and TC were mixed in the desired weight fraction and pushed into a glass tube with inside diameter 1.8 mm by a metal rod of 1.5 mm diameter. An unsintered film of polytetrafluoroethylene was used as a seal between the rod and the glass wall. The glass tube was immersed in an oil bath and the sample was melted at 190°C for 10 min. While molten, the sample was pressed with the metal rod and then cooled to room temperature at a rate of about 1.2 K min^{-1}.

The high-pressure d.t.a. apparatus used in this study has been described elsewhere[31]. Small samples cut from the rod described above were covered with aluminium foil and attached on the thermocouple junction of the high-pressure d.t.a. apparatus. High-pressure d.t.a. was performed in the following way after keeping the sample for more than 5 min at the desired pressure. Run 1 is the melting process (6 K min^{-1} heating rate) of the sample crystallized at atmospheric pressure. Run 2 is the crystallization process (5 K min^{-1} cooling rate) after reaching a temperature about 15°C higher than the peak melting temperature. Run 3 is the melting process (6 K min^{-1}) of the sample crystallized via run 2.

D.s.c. was performed on samples crystallized at atmospheric pressure and 500 MPa with a Rigaku Denki low-temperature thermal analyser at a heating rate of 5 K min^{-1}.

RESULTS AND DISCUSSION

Phase diagram

It has been reported that the endothermic melting peak of MMW PE in a mixture with TC shifted to lower temperature with decreasing W_{PE}. In the case of UHMW PE, the intensity of the melting peak also decreased and the peak position shifted to lower temperature with TC content (*Figure 1*). The peak melting temperatures of UHMW PE and TC obtained by d.s.c. measurements are plotted against weight fraction of UHMW PE in *Figure 2*. The rate of decrease of T_m for UHMW PE is nearly equal to that for MMW PE, but T_m of TC does not change with change of W_{PE}. Namely, the mixing of TC does not have a distinctly different effect on the crystallization behaviour of MMW PE and UHMW PE at atmospheric pressure.

To determine the pressure dependence of T_m of UHMW PE and TC in the mixture, high-pressure d.t.a. was performed up to 500 MPa. *Figures 3a* and *3b* show the d.t.a. melting curves of pure UHMW PE and UHMW PE in the mixture of $W_{PE} = 0.4$, respectively, at elevated pressures. As shown in *Figure 3a* for pure UHMW PE, the endothermic melting peak of folded chain crystals (FCC) of UHMW PE only shifts to higher temperature up to ~300 MPa. However, above ~300 MPa, two or three peaks appear in the melting region. In the d.t.a.

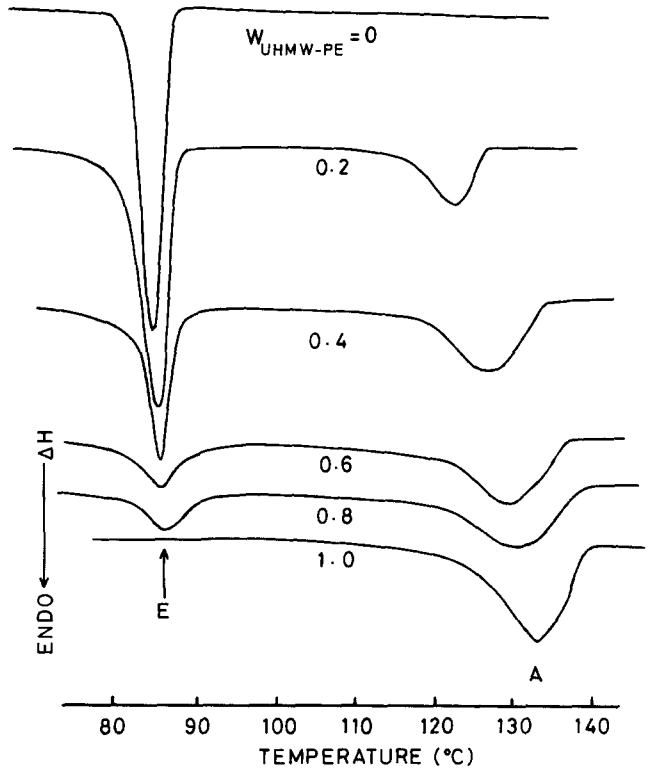

Figure 1 D.s.c. melting curves at atmospheric pressure of UHMW PE and TC binary mixture crystallized at atmospheric pressure

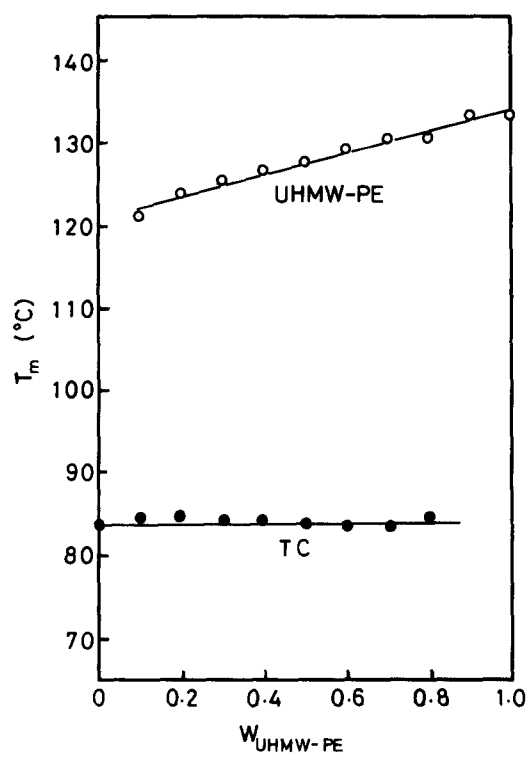

Figure 2 Phase diagram of the binary mixture of UHMW PE and TC at atmospheric pressure: (○) melting of UHMW PE; (●) melting of TC

curve at 500 MPa, three peaks (the low-, medium- and high-temperature peaks) are observed at 232.5°C (the melting of FCC), at 238.2°C (the phase transition) and at 252.7°C (the melting of the high-pressure phase), respectively. In the mixture with $W_{UHMW\,PE} = 0.4$ (*Figure 3b*), two endothermic peaks appear in the d.t.a. curve at

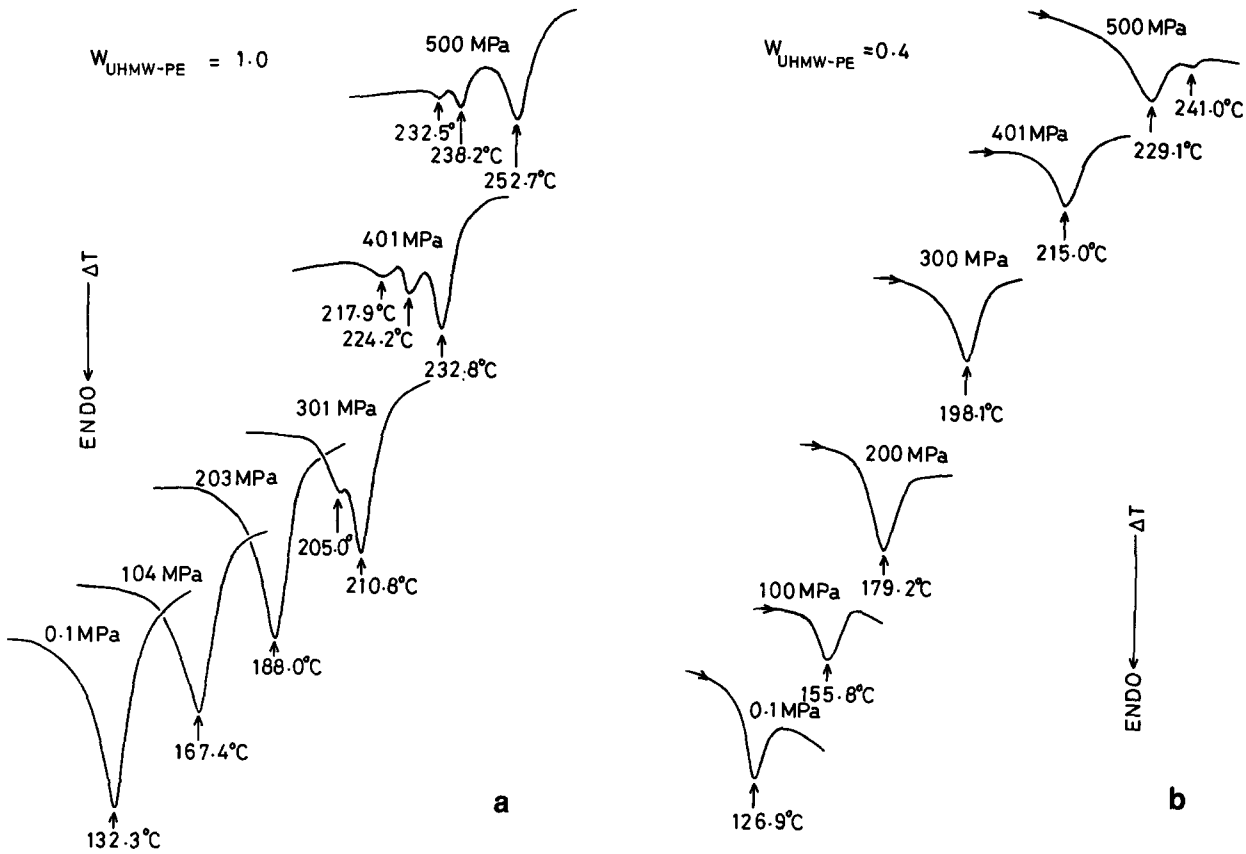

Figure 3 Pressure change of the d.t.a. melting curves (run 1) of pure UHMW PE and of UHMW PE in the binary mixture crystallized at atmospheric pressure: (a) pure UHMW PE; (b) $W_{UHMWPE} = 0.4$

500 MPa. The peak at 229.1°C is due to the melting of FCC. The small peak at 241.0°C is assigned to the melting of a small fraction of thick crystal formed during heating of FCC, on the basis of the following considerations. In run 1 of *Figure 3a* (melting of pure UHMW PE sample crystallized at atmospheric pressure), two peaks appear at 301 MPa. In this case, the low-temperature peak is due to the melting of FCC and the high-temperature peak is due to the melting of thick crystal because the peak temperature (210.8°C) is very close to the melting temperature of ECC (212.9°C) at the same pressure. Crystal thickening in PE occurs drastically above ~300 MPa during heating at a temperature close to the melting temperature[32]. It is clear that the phase transition of pure PE occurs after thick crystal is formed above ~300 MPa. The high-pressure phase in PE of $W_{UHMWPE} = 0.4$ should appear at higher pressure than 500 MPa, since the new high-temperature peak, which corresponds to the melting of ECC, begins to appear at 500 MPa. In the mixture, the critical pressure where a thick crystal begins to form is higher than the pressure in the case of pure UHMW PE.

Figure 4 shows the pressure dependence of the melting temperature of pure UHMW PE and of UHMW PE in a mixture with $W_{UHMWPE} = 0.4$. The high-pressure phase in run 1 of pure UHMW PE appears in the hatched area above 350 MPa. The pressure dependence of the melting temperature obtained from the endothermic peaks in run 1 is slightly different from those obtained from the melting peaks of ECC crystallized at 500 MPa. If crystal thickening occurs at high pressure in the heating process, the thickness of lamellae is smaller than ECC crystallized from the melt at 500 MPa. A difference in the pressure dependence of T_m between FCC and ECC was also reported in the case of MMW PE[25].

In *Figure 4*, the melting curves (T_m *versus* pressure) of the low-temperature peak of UHMW PE (○) and TC (△) in run 1 fit an equation of the form:

$$T_m = A + BP - CP^2$$

where P is the pressure. The melting curves for the other samples with different weight fractions also fit the same equation. The values of the coefficients A, B and C are determined by the least-squares method for all the mixtures and are summarized in *Table 1*. *Table 2* lists the values of the coefficients A', B' and C' for TC for the same curve fitting.

Isobaric T_m values (100 MPa each) were calculated inversely using the values of *Tables 1* and *2* and the above equation. *Figures 5a* and *5b* show the phase diagram at elevated pressures at an interval of 100 MPa. Melting-point depression of TC does not occur at pressures up to 500 MPa. For UHMW PE, the rate of depression of T_m of FCC does not change below 300 MPa, but above 400 MPa the rate decreases, and at 500 MPa depression occurs only at $W_{UHMWPE} = 0.1$. As reported in the previous paper[25], T_m of MMW PE in the mixture with TC, especially $W_{PE} < 0.5$, was depressed even at 500 MPa. These facts indicate that the solvent effect of TC for FCC of UHMW PE decreases with pressure, and the effect disappears at 500 MPa because, under such high pressure, both the intermolecular distance of PE chains and the mobility of TC should decrease. A decrease in the rate of depression of T_m was reported in poly(ε-caprolactone) in the mixture with styrene–acrylonitrile (SAN) copolymer at 500 MPa[33].

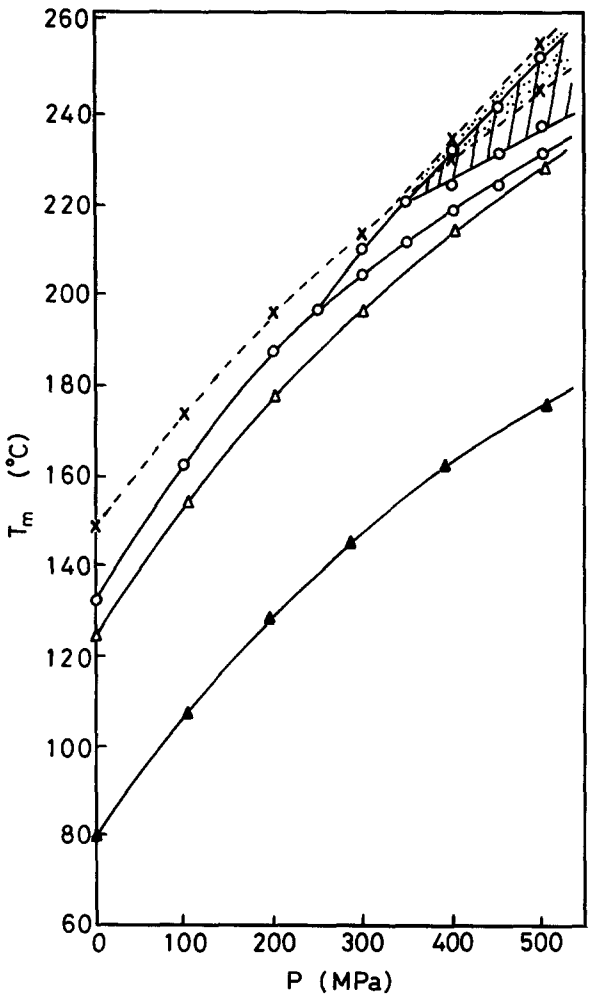

Figure 4 Pressure dependence of T_m of UHMW PE and TC in the mixture of $W_{UHMWPE} = 1.0$ and 0.4; (×) ECC in UHMW PE crystallized at 500 MPa; (○) FCC of pure PE (run 1); (△) PE in $W_{UHMWPE} = 0.4$; (▲) TC in $W_{UHMWPE} = 0.4$. The hatched area and dotted area mean the high-pressure phase of UHMW PE crystallized at atmospheric pressure and at 500 MPa, respectively

Effects of TC on the high-pressure phase of UHMW PE

Figure 6 shows the d.t.a. curves of melting and crystallization of pure UHMW PE at 500 MPa. In run 1, three peaks appear as shown in *Figure 3a*. In run 3 (melting of a pressure-crystallized sample), two peaks due to the phase transition and the melting of the high-pressure phase appear, but the low-temperature peak that appeared in run 1 is not observed. *Figure 7* shows the d.t.a. curves of melting and crystallization of UHMW PE in the mixture of $W_{UHMWPE} = 0.7$ at 500 MPa. The melting behaviour in run 1 for this sample is essentially the same as that for pure UHMW PE, but the difference between the phase transition temperature (240.4°C) and the melting temperature of the high-pressure phase (244.3°C) is smaller than in the case of pure UHMW PE. In run 3, the low-temperature peak still appears at 231.5°C. This means that a small amount of FCC is formed on UHMW PE crystallized in the mixture of $W_{UHMWPE} = 0.7$ at 500 MPa.

In the d.t.a. curve of the mixture of $W_{UHMWPE} = 0.5$, three small endothermic peaks appear in run 1, but in the mixture of $W_{UHMWPE} = 0.4$ two peaks due to the melting of FCC and thick crystal are observed at 500 MPa, as shown in *Figure 3b*. In the sample of $W_{UHMWPE} = 0.3$, two peaks appear, but for $W_{UHMWPE} =$ 0.2 and 0.1 a single melting peak of FCC corresponding to the low-temperature peaks was observed (*Figures 3a* and *3b*). Therefore, the phase transition of UHMW PE does not occur in the mixture below $W_{UHMWPE} = 0.4$. This indicates that UHMW PE in the mixture of $W_{UHMWPE} < 0.4$ melts directly without the transition even at 500 MPa. In the case of MMW PE, a d.t.a. melting curve similar to the curve for $W_{UHMWPE} = 0.4$ is observed in the mixture of $W_{PE} = 0.5$ at 500 MPa. Therefore, the effect of TC on the phase transition of UHMW PE is smaller than that of MMW PE. In a recent study, van Aerle and Lemstra[34] have suggested that entanglements existing in the fused UHMW PE were trapped in the solid state by quenching. In general, entanglements are considered to increase with the molecular weight of PE. According to Nagata *et al.*[35], the high-pressure phase of PE originates from the pressure-induced crosslinks between different molecular chains. Therefore, it is reasonable to consider that if UHMW PE contains more entanglements that remain unloosened by molten TC than MMW PE, the high-pressure phase still appears at a lower content of UHMW PE in the mixture at 500 MPa.

Table 1 Values of A, B and C in the equation

$$T_m = A + BP - CP^2$$

for the melting temperature of UHMW PE in a mixture with TC with different weight fraction in run 1 of d.t.a. up to 500 MPa. For $W_{UHMWPE} = 1.0$ and 0.4, the values are determined by the lowest-temperature peak

W_{UHMWPE}	A (°C)	B ($\times 10^{-1}$ KMPa^{-1})	C ($\times 10^{-4}$ KMPa^{-2})
1.0	133.2	3.09	2.29
0.9	131.2	3.10	2.23
0.8	131.4	3.10	2.29
0.7	128.9	3.06	2.10
0.6	129.6	3.07	2.06
0.5	130.2	3.11	2.19
0.4	127.8	2.84	1.57
0.3	126.6	3.02	1.83
0.2	127.2	2.83	1.47
0.1	124.4	2.74	1.40

Table 2 Values of A', B' and C' in the equation

$$T_m = A' + B'P - C'P^2$$

for the melting temperature of TC in a mixture with UHMW PE with different weight fraction in run 1 of d.t.a. up to 500 MPa

W_{UHMWPE}	A' (°C)	B' ($\times 10^{-1}$ KMPa^{-1})	C' ($\times 10^{-4}$ KMPa^{-2})
1.0	–	–	–
0.9	80.3	2.56	1.38
0.8	80.3	2.57	1.43
0.7	79.5	2.53	1.21
0.6	80.3	2.64	1.58
0.5	81.4	2.65	1.50
0.4	83.2	2.47	1.27
0.3	81.1	2.54	1.26
0.2	80.6	2.49	1.22
0.1	81.9	2.58	1.36
0	83.4	2.53	1.20

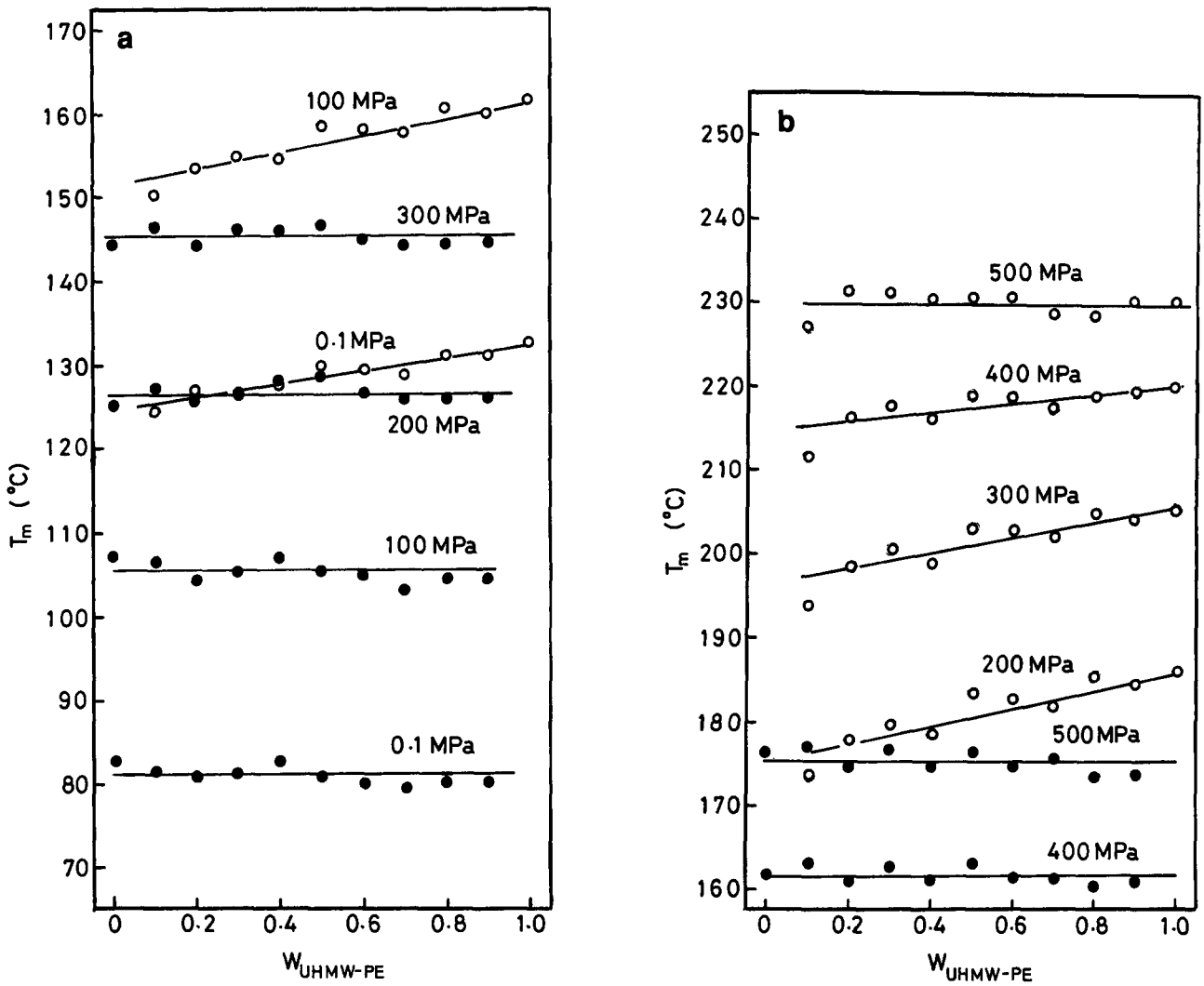

Figure 5 Phase diagram (melting) of the binary mixture of UHMW PE (○) and TC (●) with a spacing of 100 MPa: (a) lower pressure; (b) higher pressure

High-pressure crystallization of UHMW PE in the mixture

The melting behaviour of pressure-crystallized UHMW PE in the mixture is compared with the behaviour of pressure-crystallized MMW PE in the mixture.

Figure 8 shows the d.s.c. melting curves of UHMW PE and TC with different W_{UHMWPE} crystallized at 500 MPa. The d.s.c. melting curves were obtained at increments of 0.1 for W_{UHMWPE} (only alternate curves are shown for clarity). In pure UHMW PE, an endothermic peak (peak A) due to the melting of ECC is observed at 144.0°C. The low-temperature peak (peak C), which corresponds to the melting of FCC, appears for $W_{UHMWPE} \leqslant 0.8$. The lack of peak C in pressure-crystallized pure UHMW PE and in UHMW PE in the mixture of $W_{UHMWPE} = 0.9$ indicates that FCC are not formed in these samples. The intensity of peak C increases and that of ECC decreases with decreasing PE content. Below 0.3, a single melting peak of FCC is observed.

In pure MMW PE crystallized at 500 MPa, as shown in *Figure 9*, three endothermic peaks were observed in the melting: a large peak due to the melting of ECC at 141.5°C (peak A') and two small peaks at 132.8°C (peak B') and 127.0°C (peak C'), which are due to the melting of FCC. Peak A' shifted to lower temperature and peak B' shifted to higher temperature with decreasing PE content in the mixture, and they merged at $W_{MMWPE} = 0.6$. The intensity of the merged peak (peak D') decreases with TC content and disappears at $W_{UHMWPE} = 0.4$. The intensity of peak C' increased with decreasing PE content. These facts suggest that, in MMW PE, crystal thickness and content of ECC decrease with TC content in the mixture, and ECC disappear at $W_{MMWPE} = 0.5$. The amount of FCC in the mixture increases with TC content down to $W_{UHMWPE} = 0.4$ and then decreases. The peak position of peak C' of MMW PE did not change with PE content from $W_{MMWPE} = 1.0$ to 0.4, and below 0.4 it shifted to lower temperature[25]. In UHMW PE, peak A shifts to lower temperature. Its intensity decreases with decreasing UHMW PE content as already shown in *Figure 8*.

Figure 10 shows the composition dependence of the peak temperature of the d.s.c. melting curve in UHMW PE. The position of peak C did not change with W_{UHMWPE} down to 0.4, and shifted to lower temperature below $W_{UHMWPE} = 0.3$. The temperature of peak A decreases with increasing TC content. The depression of T_m of peak A is not a simple solvent effect but is due to the decrease of crystal thickness. As reported in the case

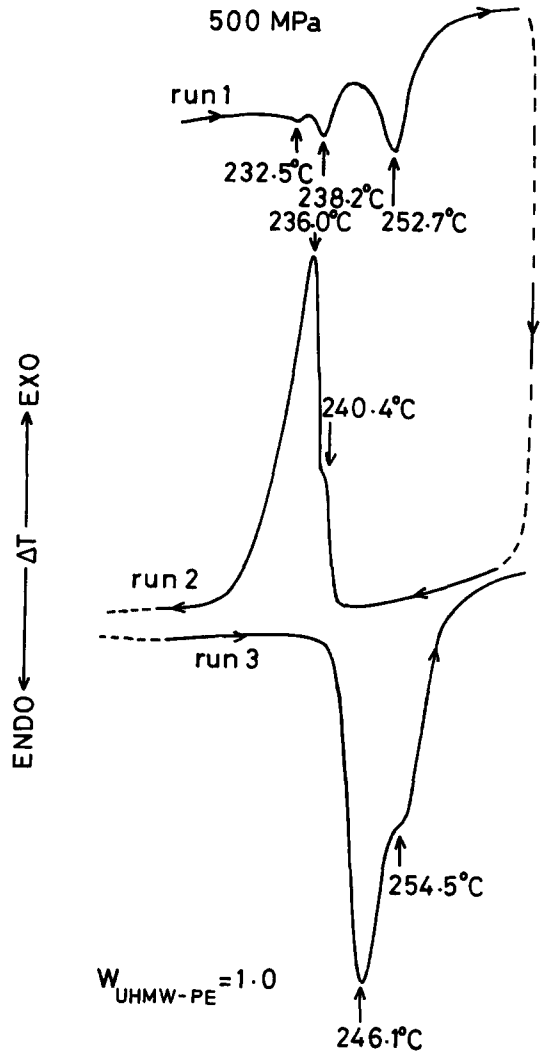

Figure 6 D.t.a. curves of melting and crystallization of pure UHMW PE ($W_{UHMWPE} = 1.0$) at 500 MPa

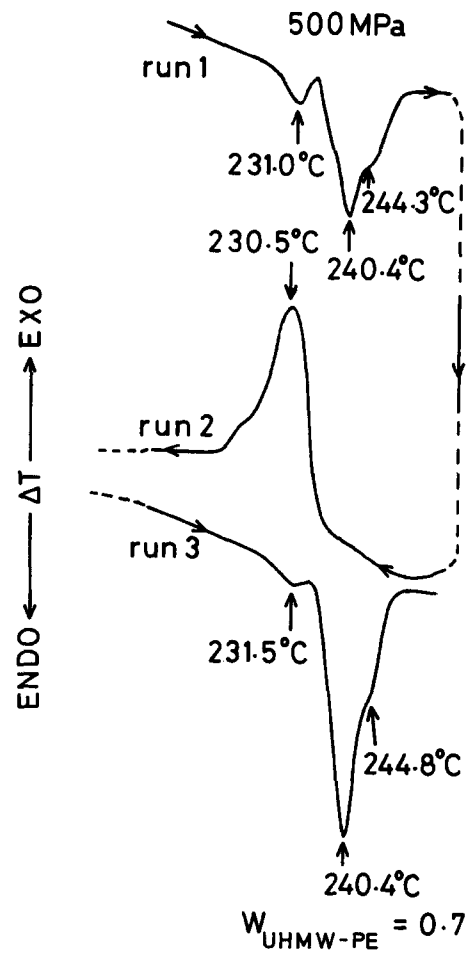

Figure 7 D.s.c. curves of melting and crystallization of UHMW PE in the binary mixture ($W_{UHMWPE} = 0.7$) at 500 MPa. Endo- and exothermic peaks due to the melting and crystallization of TC, which appear at lower temperature, are not drawn to avoid complexity

of MMW PE[25], the decrease of crystal thickness is due to the impeding effect of TC on the crystallization of PE under high pressure. It is reasonable to consider that the crystal thickness of the thick crystal formed by high-pressure crystallization decreases with TC content, taking into account that the melting peak size and position of peak A (high-temperature peak) at atmospheric pressure decrease with TC and the peak is not observed below $W_{UHMWPE} = 0.3$.

The fracture surface of pure UHMW PE crystallized at 590 MPa shows a fibrous band, which is formed by the parallel arrangement of long fibrils[26], and no FCC exist. When the crystallization of UHMW PE is performed in molten TC under high pressure, the molecular mobility of PE chains increases. Consequently, the entanglement density in UHMW PE chains should decrease. It is considered that ECC is not formed in such a state of increased molecular mobility even at 500 MPa. The absence of the medium-temperature peak is also interpreted by the above mechanism.

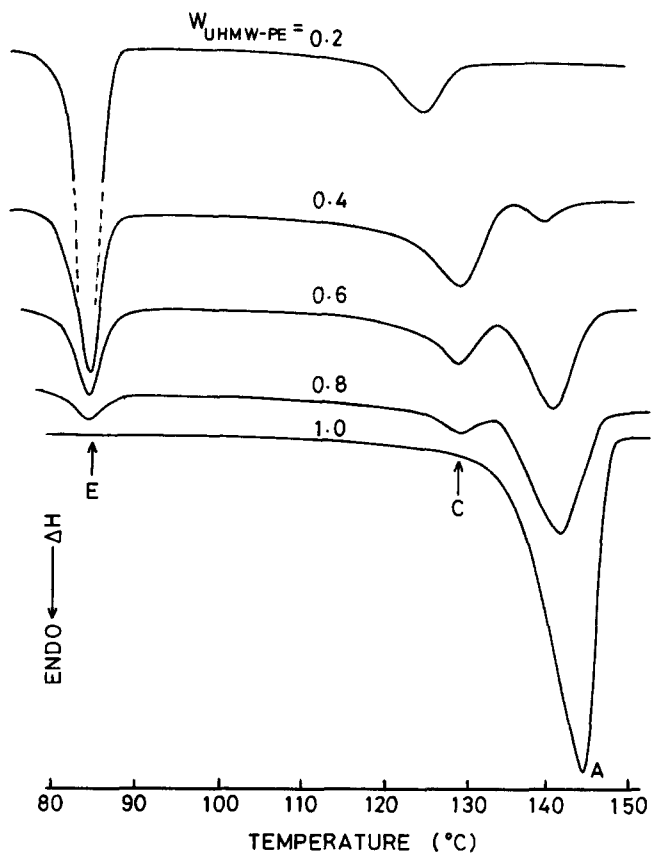

Figure 8 D.s.c. melting curves at atmospheric pressure of UHMW PE (peaks A and C) and TC (peak E) binary mixture crystallized at 500 MPa

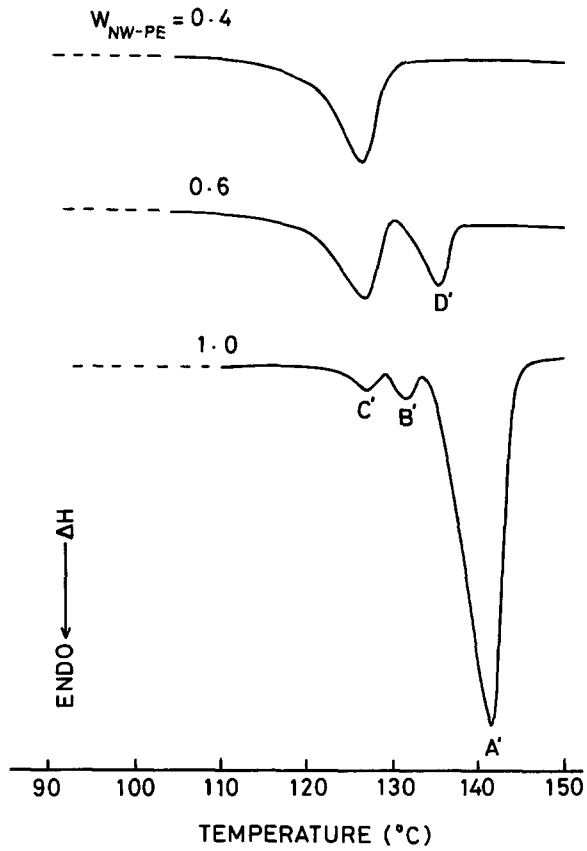

Figure 9 D.s.c. melting curves at atmospheric pressure of MMW PE and TC binary mixture crystallized at 500 MPa. Melting peak of TC is neglected

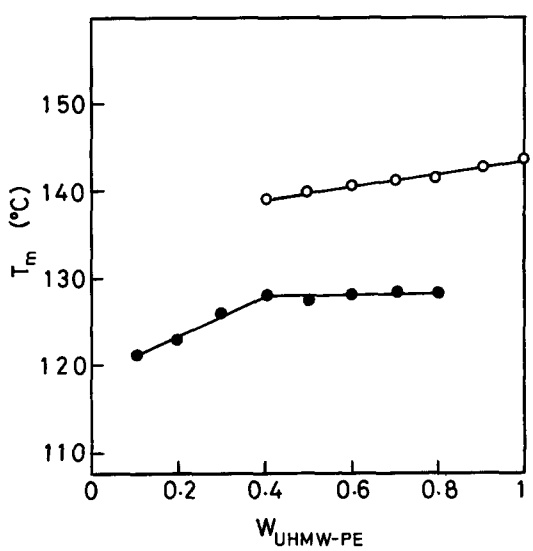

Figure 10 Composition dependence of T_m of UHMW PE crystallized at 500 MPa from d.s.c. curve in *Figure 8*: (○) high-temperature peak (peak A); (●) low-temperature peak (peak C)

CONCLUSIONS

The phase diagram of the binary mixture of UHMW PE and TC was deduced from the melting temperature at elevated pressure. Melting-point depression of UHMW PE occurs with increasing TC content at atmospheric pressure. However, it does not occur at 500 MPa due to the decreased solvent effect of TC.

The high-pressure phase was observed above 350 MPa in pure UHMW PE and in UHMW PE in mixtures of weight fraction of PE above 0.5, but it disappears in mixtures below the weight fraction of PE of 0.4.

The high-pressure crystallization of UHMW PE in mixtures of $W_{UHMW\,PE} = 0.9$ and 1.0 results in the formation of only ECC, but in mixtures below $W_{UHMW\,PE} = 0.8$ FCC are formed even in crystallization at 500 MPa.

The solvent effect of TC on the melting of solid UHMW PE almost disappears at 500 MPa. However, the effect of TC on ECC formation is remarkable.

REFERENCES

1 Bassett, D. C. and Turner, B. *Nature (Phys. Sci.)* 1972, **240**, 1468
2 Yasuniwa, M., Nakafuku, C. and Takemura, T. *Polym. J.* 1973, **4**, 526
3 Bassett, D. C. and Turner, B. *Phil. Mag.* 1974, **29**, 285
4 Bassett, D. C. and Turner, B. *Phil. Mag.* 1974, **29**, 925
5 Bassett, D. C., Block, S. and Piermarini, G. J. *J. Appl. Phys.* 1974, **45**, 4146
6 Yasuniwa, M., Enoshita, R. and Takemura, T. *Jpn. J. Appl. Phys.* 1976, **15**, 1421
7 Yamamoto, T., Miyaji, H. and Asai, K. *Jpn. J. Appl. Phys.* 1977, **16**, 1891
8 Hikosaka, M., Minomura, S. and Seto, T. *Jpn. J. Appl. Phys.* 1980, **19**, 1763
9 Tanaka, H. and Takemura, T. *Polym. J.* 1980, **12**, 335
10 Wunderlich, B. 'Macromolecular Physics', Academic Press, New York, 1980, Vol. 3
11 Hikosaka, M. *Jpn. J. Appl. Phys.* 1981, **20**, 617
12 Maeda, Y., Kanetsuna, H., Nagata, K., Matsushige, K. and Takemura, T. *J. Polym. Sci., Polym. Phys. Edn.* 1981, **19**, 1313
13 Bassett, D. C. 'Principles of Polymer Morphology', Cambridge University Press, Cambridge, 1981
14 Bassett, D. C. 'Developments in Crystalline Polymers-1', Applied Science, London, 1982, Ch. III
15 Asahi, T. *J. Polym. Sci., Polym. Phys. Edn.* 1984, **22**, 175
16 Wunderlich, B. and Arakawa, T. *J. Polym. Sci. (A)* 1964, **2**, 3697
17 Geil, P. H., Anderson, F. R., Wunderlich, B. and Arakawa, T. *J. Polym. Sci. (A-2)* 1964, **2**, 3707
18 Wunderlich, B. and Melillo, L. *Makromol. Chem.* 1968, **228**, 250
19 Wunderlich, B. and Davidson, T. *J. Polym. Sci. (A-2)* 1969, **7**, 2043
20 Prime, R. B. and Wunderlich, B. *J. Polym. Sci. (A-2)* 1969, **7**, 2061
21 Prime, R. B. and Wunderlich, B. *J. Polym. Sci. (A-2)* 1969, **7**, 2073
22 Prime, R. B., Wunderlich, B. and Melillo, L. *J. Polym. Sci. (A-2)* 1969, **7**, 2091
23 Wunderlich, B. 'Macromolecular Physics', Academic Press, New York, 1973, Vol. 3, p. 217
24 Hikosaka, M. *Polymer* 1987, **28**, 1257
25 Nakafuku, C., Yasuniwa, M. and Tsubakihara, S. *Polym. J.* 1990, **22**, 110
26 Yasuniwa, M., Haraguchi, K., Nakafuku, C. and Hirakawa, S. *Polym. J.* 1985, **17**, 1209
27 Yasuniwa, M. and Nakafuku, C. *Polym. J.* 1987, **19**, 805
28 Yasuniwa, M., Tsubakihara, S. and Nakafuku, C. *Polym. J.* 1988, **20**, 1075
29 Nakajima, A. and Hamada, F. *Kolloid Z. Z. Polym.* 1965, **205**, 55
30 Organ, S. J. and Keller, A. *J. Polym. Sci. (B) Polym. Phys.* 1986, **24**, 2319
31 Nakafuku, C. *Polym. J.* 1985, **17**, 869
32 Yasuniwa, M. and Tsubakihara, S., in preparation
33 Nakafuku, C. *Polym. J.* 1989, **21**, 781
34 van Aerle, N. A. J. M. and Lemstra, P. J. *Polym. J.* 1988, **20**, 131
35 Nagata, N., Tagashira, K., Taki, S. and Takemura, T. *Jpn. J. Appl. Phys.* 1980, **19**, 985